Feedback control of Rabi oscillations in circuit QED

Wei Cui[1] and Franco Nori[1,2]
[1]*CEMS, RIKEN, Saitama 351-0198, Japan*
[2]*Physics Department, The University of Michigan, Ann Arbor, Michigan 48109-1040, USA*
(Received 30 April 2013; published 10 December 2013)

We consider the feedback stabilization of Rabi oscillations in a superconducting qubit which is coupled to a microwave readout cavity. The signal is readout by homodyne detection of the in-phase quadrature amplitude of the weak-measurement output. By multiplying the time-delayed Rabi reference, one can extract the signal, with maximum signal-to-noise ratio, from the noise current. We further track and stabilize the Rabi oscillations by using Lyapunov feedback control to properly adjust the input Rabi drives. Theoretical and simulation results illustrate the effectiveness of the proposed control law.

DOI: 10.1103/PhysRevA.88.063823 PACS number(s): 42.50.Pq, 42.50.Dv, 85.25.−j

I. INTRODUCTION

In control theory, the system to be controlled is compared to the desired reference, and the discrepancy is used to modify the control action [1]. In contrast to classical systems, where measurements do not alter the state of the system, quantum measurements will collapse the system instantaneously into one of its eigenstates in a probabilistic manner: the "measurement-induced backaction" [2,3]. Although quantum coherent feedback control has been proposed [4] and extensively applied in quantum optics and for cooling mechanical oscillators [5–7], measurement-based feedback control still attracts considerable interest. Based on the quantum trajectory theory, Wiseman and Milburn [8,9] developed a quantum conditional stochastic master equation (SME) to describe the dynamics resulting from the feedback (of the measurement output at each instant) to the quantum system. SME has been a topic of considerable activity in recent years for it paves the way for studying real-time measurement-based feedback control [10–14] in quantum information processing and computation.

Circuit quantum electrodynamics (i.e., circuit QED, where a superconducting qubit is coupled to a microwave-frequency resonator cavity; see, e.g., Refs. [15–19]) has been shown to be a promising quantum computing architecture. Circuit QED allows for rapid, repeated quantum nondemolition (QND) superconducting qubit measurement [2,20,21] and also provides several simple high-fidelity readout mechanisms, such as using large measurement drive powers [22], and using either quantum-limited [23] or nonlinear bifurcation amplifiers [24]. Moreover, circuit QED is an excellent test bed for implementing quantum feedback control in either the qubits or the microwave resonator [25–32]. For example, a recent work [33] verified that measurement-based feedback using continuous weak measurement of a qubit can reduce dephasing and remarkably prolong Rabi oscillations. The method they proposed and verified is based on the quantum Bayesian formalism. Based on the phase-shift error $\eta_{\rm err}$, they define the direct-feedback control law $\Omega_{\rm fb}(t)$ to compensate the dephasing (Eq. (12) in the supplementary information of Ref. [33]). Another protocol to stabilize any trajectory of a single qubit using a stroboscopic digital feedback based on strong quantum measurement was proposed in [34] and experimentally verified in [35]. They proposed using two feedback loops to obtain persistent Rabi oscillations in circuit QED: The first one is to correct the phase diffusion of the Rabi oscillations by applying corrective π pulses, and the second one is used to compensate the deviation in the amplitudes [34].

In our work, we propose an alternative feedback phase-correction scheme. The method used here is the Lyapunov-function method. This method is widely used in stability and control theory. Based on this approach, we analytically derive a simple and experimentally feasible measurement-based feedback control law for circuit QED to track and stabilize Rabi oscillations. Moreover, we prove that, with the help of this control law, the extracted signal will asymptotically converge to the reference signal. The main results in our study are the following. First, in a general sense, the proposed Lyapunov-function method contributes not only to the Rabi stabilization, but also applies to several other examples of physical interest (including, e.g., quantum state preparation and purification). Second, the Lyapunov feedback method is valid to track any trajectory and admits a precise convergence analysis. Third, we studied in detail the single-qubit readout by measuring the state of the emitted microwave field. We also discussed the connection between information gain and dephasing via an effective stochastic master equation for the qubit degree of freedom. Furthermore, our work might help realize high-fidelity measurements for both single-qubit [30,36] and joint measurements of two qubits [37], and better understand the fundamental limits of quantum state estimation [38–41].

The paper is organized as follows. The next section contains a brief discussion of the circuit QED Hamiltonian, the quantum detection, and the stochastic master equation for the qubit. In Sec. III, we study the open-loop control of Rabi oscillations. In Sec. IV, we study the feedback control by the Lyapunov function method. We summarize our conclusions in Sec. V.

II. CIRCUIT FOR MEASUREMENT AND FEEDBACK CONTROL

As shown in Fig. 1(a), we consider a superconducting circuit QED system with a superconducting qubit coupled to a microwave readout cavity and driven by two external drives: (i) a readout drive with amplitude $\epsilon_d(t)$ and frequency ω_d near the cavity resonance frequency ω_c, and (ii) a Rabi drive with amplitude $\epsilon_r(t)$ and frequency ω_r near the frequency of the

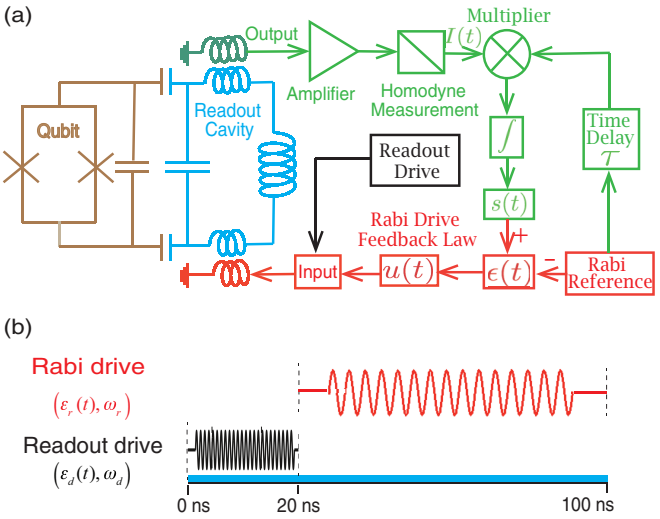

FIG. 1. (Color online) (a) Simplified circuit diagram of measurement and feedback control. A superconducting qubit (brown) is coupled to a microwave readout detector cavity (blue). The amplified output is homodyne detected and the quadrature signal (green) is then extracted from the noise current $I(t)$ by multiplying the time-delayed Rabi reference. The discrepancy is used to design the feedback-control law to correct Rabi oscillations (red). (b) Schematic of the readout drive to build up the photon population of the cavity and Rabi drive to stabilize the Rabi oscillation.

qubit ω_q [24,33,42,43]. The Hamiltonian of the entire system can be written as

$$H = \hbar\omega_c a^\dagger a + \hbar\frac{\omega_q}{2}\sigma_z + \hbar g(a^\dagger\sigma_- + a\sigma_+) + \hbar[\epsilon_d(t)e^{-i\omega_d t}a^\dagger + \epsilon_r(t)e^{-i\omega_r t}a^\dagger + \text{H.c.}], \quad (1)$$

where $a^\dagger$ and a are the creation and annihilation operators for the microwave readout cavity, σ_+ and σ_- are the raising and lowering operators of the superconducting qubit, and g is the coupling strength between the cavity and the qubit. In the dispersive regime [44,45], $|\Delta| = |\omega_q - \omega_c| \gg g$, by applying the dispersive shift $U = \exp[g(a\sigma_+ - a^\dagger\sigma_-)/\Delta]$, and moving to the rotating frames for both the qubit and cavity, $U_c = \exp(ia^\dagger a\omega_d t)$, $U_q = \exp(i\sigma_z\omega_r t/2)$, with the rotating-wave approximation, the Hamiltonian in Eq. (1) becomes

$$H_{\text{eff}} = \hbar\Delta_c a^\dagger a + \hbar\chi a^\dagger a\sigma_z + \hbar\frac{\tilde{\omega}_q}{2}\sigma_z + \hbar\frac{\Omega_R}{2}\sigma_x + \hbar(\epsilon_d + \epsilon_r)(a^\dagger + a), \quad (2)$$

where

$$\Delta_c = \omega_c - \omega_d, \quad \chi = g^2/\Delta, \quad \Omega_R = 2\epsilon_r(t)g/\Delta, \quad (3)$$

and the Lamb-shifted qubit transition frequency

$$\tilde{\omega}_q = \omega_q - \omega_r + \chi. \quad (4)$$

If the cavity state is coherent, and the microwave cavity decay rate is much larger than the qubit decay rate, $\kappa \gg \gamma_1$ (that allows one to decouple the qubit dynamics from the resonator adiabatically), the state at time t is given by $|g\rangle \otimes |\alpha_g(t)\rangle$ or $|e\rangle \otimes |\alpha_e(t)\rangle$. Here $|\alpha_{g(e)}(t)\rangle$ are coherent states of the cavity and, from Eq. (2), the field amplitudes are given by [46]

$$\dot{\alpha}_g(t) = -i\epsilon_d(t) - i(\Delta_c - \chi)\alpha_g(t) - \frac{\kappa}{2}\alpha_g(t),$$
$$\dot{\alpha}_e(t) = -i\epsilon_d(t) - i(\Delta_c + \chi)\alpha_e(t) - \frac{\kappa}{2}\alpha_e(t). \quad (5)$$

Thus, these coherent states $\alpha_{g(e)}$ act as "pointer states" [9] for the qubit. Based on homodyne detection, by applying the transformation

$$P(t) = |e\rangle\langle e|D[\alpha_e(t)] + |g\rangle\langle g|D[\alpha_g(t)], \quad (6)$$

with $D[\alpha] = \exp(\alpha a^\dagger - \alpha^* a)$ as the displacement operator of the microwave cavity, the effective stochastic master equation [46] for the qubit degrees of freedom becomes

$$d\tilde{\rho} = -\frac{i}{\hbar}\frac{\tilde{\omega}_{ac}(t)}{2}[\sigma_z, \tilde{\rho}]dt - i\frac{\Omega_R}{2}[\sigma_x, \tilde{\rho}]dt + \gamma_1\mathcal{D}[\sigma_-]\tilde{\rho}dt + \frac{\gamma_\phi + \Gamma_d(t)}{2}\mathcal{D}[\sigma_z]\tilde{\rho}dt + \sqrt{\kappa\eta}|\beta(t)|\mathcal{H}[\sigma_z]\tilde{\rho}dW_t. \quad (7)$$

The only difference between this control master equation and the general master equation for circuit QED is the driving term $\epsilon_r \exp(-i\omega_r t)a^\dagger + \text{H.c.}$ in Eq. (1). Applying the dispersive shift U to this term, it becomes $\epsilon_r \exp(-i\omega_r t)(a^\dagger + g\sigma_+/\Delta) + \text{H.c.}$ Here, the Rabi drive $\frac{\Omega_R}{2}(\sigma_- e^{i\omega_r t} + \sigma_+ e^{-i\omega_r t})$ plays an important role. Based on the Rabi drive Hamiltonian, the master equation with Rabi drive was derived in Eq. (C7) of Ref. [46].

In the stochastic master equation (7)

$$\tilde{\omega}_{ac}(t) = \tilde{\omega}_q + B(t), \quad (8)$$

and

$$\beta(t) = \alpha_e(t) - \alpha_g(t) \quad (9)$$

is the separation between the pointer states $\alpha_g(t)$ and $\alpha_e(t)$, η is the measurement efficiency, γ_ϕ is the pure dephasing rate, $\mathcal{D}[A]$ is the damping superoperator

$$\mathcal{D}[A]\rho = A\rho A^\dagger - \tfrac{1}{2}(A^\dagger A\rho + \rho A^\dagger A), \quad (10)$$

and

$$\mathcal{H}[A]\tilde{\rho} = A\tilde{\rho} + \tilde{\rho}A^\dagger - \langle A + A^\dagger\rangle\tilde{\rho}. \quad (11)$$

Also,

$$\Gamma_d(t) = 2\chi\,\text{Im}[\alpha_g(t)\alpha_e^*(t)] \quad (12)$$

is the measurement-induced dephasing and

$$B(t) = 2\chi\,\text{Re}[\alpha_g(t)\alpha_e^*(t)] \quad (13)$$

is the ac Stark shift [37,46]. The innovation dW_t is a Wiener process [9] with

$$E[dW_t] = 0 \quad \text{and} \quad E\left[dW_t^2\right] = dt. \quad (14)$$

Due to the qubit decay γ_1 and dephasing $\gamma_\phi + \Gamma_d(t)$, the quantum system will eventually lose its coherence.

A coherent drive is turned on for 20 ns to build up the photon population of the cavity and is then repeated every 100 ns [see Fig. 1(b)]. The cavity pull $\chi/2\pi$ represents the dispersive coupling strength between the cavity photon number and the qubit [46,47]. We choose a cavity pull $\chi/2\pi = 5$ MHz, and cavity decay rate $\kappa/2\pi = 20$ MHz. A homodyne detection

of the readout cavity field, with the help of the distance $\beta(t)$ between the states $|\alpha_e(t)\rangle$ and $|\alpha_g(t)\rangle$, can then be used to distinguish the coherent states and thus readout the state of the qubit. By applying the P transformation to the in-phase quadrature amplitude

$$I_\phi = \tfrac{1}{2}(ae^{-i\phi} + a^\dagger e^{i\phi}), \tag{15}$$

with ϕ the phase of the local oscillation, the homodyne measurement record from the microwave cavity becomes

$$I(t) = \sqrt{\kappa\eta}|\beta(t)|\langle\sigma_z(t)\rangle + \xi(t) = s(t) + \xi(t), \tag{16}$$

where the qubit uncorrelated term $\sqrt{\kappa\eta}|\mu(t)|\sin[\phi + \arg(\mu)]$, with $\mu = \alpha_g + \alpha_e$, has been omitted. We have set the homodyne phase ϕ to arg β, which corresponds to detecting the quadrature with the greatest separation of the pointer states. Here $\xi(t) = dW_t/dt$ is a Gaussian white noise, representing the shot noise, with spectral density $P_\xi(\omega) = 1$. We now face the challenge of detecting a signal $s(t)$ which is smaller than the noise $\xi(t)$, because the signal-to-noise ratio $S/N < 1$ (S/N is defined in the Appendix). The overall objective now is to make the system behave in a desired way by manipulating the input drive based on the measurement output. This feedback strategy could extend the number of Rabi oscillations. To achieve this, the following steps are required: (a) detect the signal $s(t)$ from the noise current $I(t)$; (b) reconstruct $x_1(t) = \mathrm{Tr}\,[\sigma_x\tilde{\rho}(t)]$, $x_2(t) = \mathrm{Tr}\,[\sigma_y\tilde{\rho}(t)]$, and $x_3(t) = \mathrm{Tr}\,[\sigma_z\tilde{\rho}(t)]$, which are the three components of the Bloch vector for the ensemble qubit state based on the detected signal [48]; (c) feedback the error signal between the reconstructed state and the desired state, to design the feedback control law (the Rabi drive), thus minimizing the error.

III. OPEN-LOOP CONTROL: NO FEEDBACK

To see how the feedback Rabi drive will work, we first consider the open-loop control. Open loop [49,50] means that we do not use feedback to determine if the output has achieved the desired goal. One can simply drive the microwave cavity with amplitude

$$\epsilon_r = \frac{1}{2g}\Omega_R\Delta \tag{17}$$

to obtain Rabi oscillations with frequency Ω_R; but cannot correct any errors. To illustrate this, we have numerically simulated the microwave cavity field equation (5) and the superconducting qubit stochastic master equation (7) with the open-loop drive (17) to obtain the expected frequency $\Omega_R/2\pi = 1$ MHz, for four different measurement drives.

In Fig. 2, we numerically analyze the Rabi oscillations by the open-loop control with frequency $\Omega_R/2\pi = 1$ MHz. We set the initial state of the qubit as the excited state. In these results we set the measurement efficiency $\eta = 1$, the qubit decay $\gamma_1/2\pi = 0.05$ MHz, and the pure dephasing rate $\gamma_\phi/2\pi = 0.1$ MHz. The Rabi-drive amplitude ϵ_r and the frequency $\omega_r = \omega_q + \chi$, should be chosen carefully to make the Lamb-shifted qubit transition frequency equal zero.

When acquiring information from the measurement, it of course induces significant backaction on the system. From Fig. 2(a), we see that for the small measurement-drive amplitude ($\epsilon_d/2\pi = 1$ MHz, red solid curve), the qubit decays

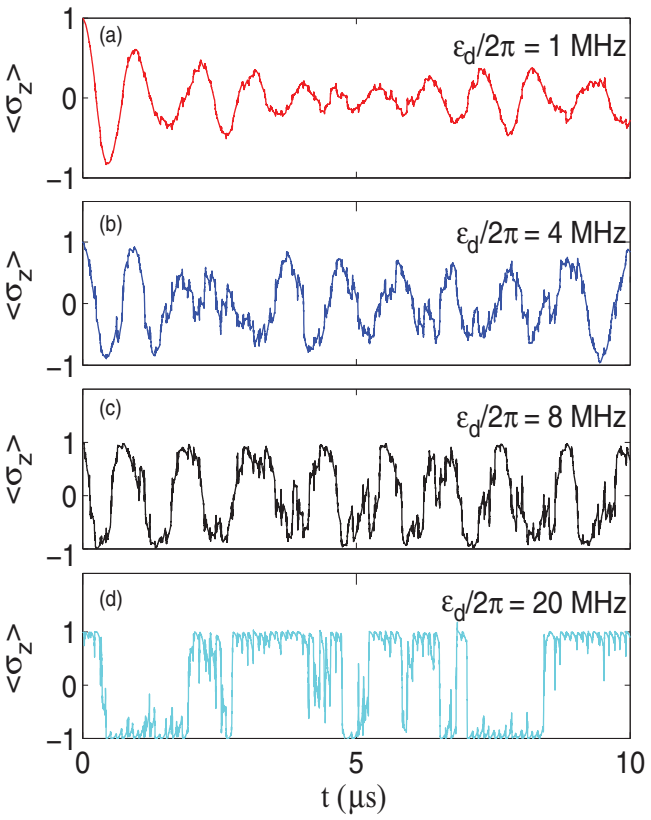

FIG. 2. (Color online) Evolution of the conditional state [here we only plot $\langle\sigma_z(t)\rangle$] by continuous weak measurements of the open-loop controlled microwave readout cavity with Rabi frequency $\Omega_R/2\pi = 1$ MHz. The Rabi-drive amplitude $\epsilon_r = \Omega_R\Delta/2g$ and the frequency $\omega_r = \omega_q + \chi$, which makes the Lamb-shifted qubit transition frequency equals zero. The qubit is initially in the excited state and the readout drive amplitudes are $\epsilon_d/2\pi = 1$ MHz (a), 4 MHz (b), 8 MHz (c), and 20 MHz (d), respectively.

and pure dephasing dominates the evolution. Thus, in this case, the measurement only causes small amplitude noise on the Rabi oscillation. However, for the larger drive amplitudes $\epsilon_d/2\pi = 4$ MHz [Fig. 2(b)] and 8 MHz [Fig. 2(c)] the measurements induce backaction on the qubit.

We now set $\epsilon_d/2\pi = 20$ MHz to gain more insight into what is happening during the evolution of the Rabi oscillation with strong measurement-drive amplitude. As shown in Fig. 2, $\langle\sigma_z\rangle$ exhibits decaying oscillations, in Figs. 2(a)–2(c), when the drive is weak ($\epsilon_d/2\pi = 1$, 4, and 8 MHz) and discontinuous jumps between two levels, in Fig. 2(d), when the driving is strong ($\epsilon_d/2\pi = 20$ MHz). Clearly, in the strong drive, the qubit will remain fixed at either $z = +1$ or -1. This is the Zeno effect. Thus, Fig. 2 shows that open-loop control cannot compensate for disturbances in the system.

IV. FEEDBACK CONTROL

Based on the above measurement procedures, we now propose a simple feedback-control law allowing one to compensate the dephasing of the superconducting qubit, the measurement-induced backaction, and to maintain the coherence of the Rabi oscillations. The schematics of such feedback control is shown in Fig. 1. The amplified and filtered

signal $s(t) = \langle \sigma_z(t) \rangle$ is compared with the Rabi reference signal $s^*(t) = \cos\ \Omega_R^0 t$, and the difference

$$\varepsilon(t) = s(t) - s^*(t) \tag{18}$$

is used to generate the feedback signal $u(t)$ that drives the microwave cavity in order to reduce the difference with the desired Rabi oscillations: $\varepsilon(t) \to 0$ (frequency tracking [51]). The difference $\varepsilon(t)$ evolves as

$$\begin{aligned} \dot{\varepsilon}(t) &= \dot{s}(t) - \dot{s}^*(t) \\ &= E\left[\frac{d}{dt}\langle \sigma_z(t) \rangle\right] - \dot{s}^*(t) \\ &= \Omega_R(t)\langle \sigma_y(t) \rangle - \gamma_1[1 + \langle \sigma_z(t) \rangle] + \Omega_R^0 \sin\ \Omega_R^0 t. \end{aligned} \tag{19}$$

Thus, we design the feedback control law (the Rabi-drive amplitude):

$$\begin{aligned} u(t) &= \epsilon_r(t) \\ &= -\frac{\Delta}{2g}\langle \sigma_y(t) \rangle^{-1}\big[K_1\ \mathrm{sgn}\,\varepsilon(t) + K_2\varepsilon(t) \\ &\quad - \gamma_1[1 + \langle \sigma_z(t) \rangle] + \Omega_R^0 \sin\ \Omega_R^0 t\big], \end{aligned} \tag{20}$$

where $K_1, K_2 > 0$. Using the feedback-control law (20) in Eq. (19), we have

$$\dot{\varepsilon}(t) = -K_1\ \mathrm{sgn}\ \varepsilon(t) - K_2\varepsilon(t). \tag{21}$$

Clearly, if $\varepsilon(t) > 0$, then $\dot{\varepsilon}(t) < 0$; and if $\varepsilon(t) < 0$, then $\dot{\varepsilon}(t) > 0$.

The Lyapunov function method [52–57] is employed to prove the stability of an ordinary differential equation and widely used in stability and control theory. Here we can choose a simple Lyapunov function

$$v(t) = \tfrac{1}{2}\varepsilon^2(t). \tag{22}$$

Obviously,

$$v(t) > 0 \quad \text{and} \quad \dot{v}(t) = \dot{\varepsilon}(t)\varepsilon(t) < 0. \tag{23}$$

Then, the Lyapunov theorem tells us that every trajectory of Eq. (18) converges to zero:

$$\lim_{t\to\infty} |s(t) - s^*(t)| \to 0 \quad \text{as} \quad t \to \infty, \tag{24}$$

which means the system is globally asymptotically stable. Now, the only problem is to choose suitable values of K_1 and K_2. From the feedback control law in Eq. (20), we find that when $s(t)$ is far from $s^*(t)$, a large K_2 is needed to make $s(t)$ quickly converge to $s^*(t)$. If $s(t)$ is quite close to $s^*(t)$, $\mathrm{sgn}\,\varepsilon(t)$ dominates the evolution, thus a small K_1 is needed to reduce the error $\varepsilon(t)$. Note that the feedback control law (20) corresponds to the amplitude of the Rabi drive. In practice, $u(t)$ must be finite and, thus, $\langle \sigma_y \rangle$ must be nonzero. When $\langle \sigma_y \rangle = 0$, a maximum cutoff on $u(t)$ must be imposed. In the simulation, the function $u(t)$ in Eq. (20) is $\sim 10^6$. At the nine points where $\langle \sigma_y \rangle = 0$, we impose a cutoff of the amplitude $|\langle \sigma_y \rangle| = 2 \times 10^7$. We further compared this to a much larger cut-off value $|\langle \sigma_y \rangle| = 10^8$, and we found that it made no difference to our results (Fig. 3).

We have simulated the feedback loop designed above to maintain Rabi oscillations with frequency $\Omega_R^0/2\pi = 2.5$ MHz. The measurement is set in the weak-driving regime, when the readout drive amplitude is $\epsilon_d/2\pi = 1$ MHz, where the measurement-induced backaction $\Gamma_d(t)$ and $B(t)$ are small. The control parameters used here are $K_1 = 5 \times 10^6$ and $K_2 = 10^8$. The other parameters are the same as in the case of open-loop control. Figure 3(a) shows typical realizations of the feedback-controlled ensemble-averaged Rabi oscillations. Clearly, the feedback control can quickly track the reference Rabi signal and ideally fight against dephasing and the measurement-induced backaction. From Fig. 3 we can see that the feedback-controlled Rabi oscillations persist for much longer time than those with open-loop control. Finally, in Fig. 3(b), we compare the power spectral density of the averaged measurement record in feedback-controlled Rabi oscillations (red curve) with the corresponding open-loop control (blue curve). Both of them are centered at 2.5 MHz. However, the feedback-controlled spectrum has a sharp peak at the Rabi reference frequency, while the open-loop controlled spectrum has a broad distribution. Clearly, for stabilizing the Rabi oscillations in circuit QED, the proposed feedback control has more advantages than the open-loop control.

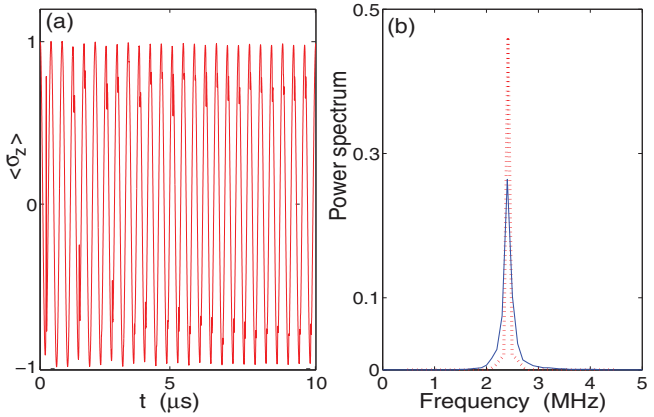

FIG. 3. (Color online) (a) Feedback-controlled ensemble-averaged (over 1,000 realizations) Rabi oscillations, which persist for much longer time than those with open-loop control. The Rabi frequency $\Omega_R^0/2\pi = 2.5$ MHz and the read-out drive amplitude is $\epsilon_d/2\pi = 1$ MHz. (b) Power spectral density for the averaged measurement of feedback-controlled Rabi oscillations from (a) (red curve); the blue curve corresponds to the open-loop case with the same parameters of (a).

V. CONCLUSION

In conclusion, we have proposed a feedback phase-correction scheme based on the Lyapunov-function method to stabilize the Rabi oscillations in a superconducting qubit which is coupled to a microwave readout cavity. Based on this approach, we analytically derived a simple and experimentally feasible measurement-based feedback control law for circuit QED to track and stabilize Rabi oscillations. Moreover, with the help of this control law, we proved that the extracted signal will asymptotically converge to the reference signal. Thus, we can precisely convert the amplitude of the resonator microwave drive to the frequency of the induced Rabi oscillations, which can be understood as an amplitude-to-frequency converter.

To use the Lyapunov feedback control [52–58] one needs to construct an artificial closed-loop controller first, simulate it, and then obtain the open-loop controller by the simulation results. During this process, a suitably chosen Lyapunov function is monotonically decreasing along every trajectory. A number of Lyapunov feedback-control designs have been proposed and numerous results established (including, e.g., quantum state preparation [55], quantum decoherence control [56], cooling of a mechanical oscillator [57], and quantum state feedback stabilization [58]). Mathematically, if the desired final state is $|\psi\rangle_t$, by using the Lyapunov feedback control, one can choose the Lyapunov function $v(t) = \frac{1}{2}(1 - |\langle\psi_t|\psi\rangle|^2)$ and construct the control law to guarantee that $\frac{d}{dt}v(t) \leqslant 0$. Reference [55] demonstrated that the Lyapunov feedback control can make the quantum system converge from any initial state to the target state. Recently, optimal Lyapunov feedback control was further proposed to shorten the time required to reach the target state [57].

ACKNOWLEDGMENTS

The authors would like to thank the referees for their valuable comments and suggestions. W.C. would like to thank Dr. J. Q. Liao, Dr. W. D. Oliver, and Dr. M. Tsang for helpful comments. W.C. is supported by the RIKEN FPR Program. F.N. is partially supported by the ARO, RIKEN iTHES Project, MURI Center for Dynamic Magneto-Optics, JSPS-RFBR Contract No. 12-02-92100, a Grant-in-Aid for Scientific Research (S), MEXT "Kakenhi on Quantum Cybernetics," and the JSPS via its FIRST program.

APPENDIX: QUADRATURE SIGNAL EXTRACTED FROM THE NOISE

To detect the signal $s(t)$ from the noise current $I(t)$ one needs to design the impulse response $h(t)$ of the filter. The output of the filter can be expressed as

$$\begin{aligned} y(t) &= \int_{-\infty}^{\infty} h(t-\tau)I(\tau)d\tau \\ &= \int_{-\infty}^{\infty} h(t-\tau)s(\tau)d\tau + \int_{-\infty}^{\infty} h(t-\tau)\xi(\tau)d\tau \\ &\equiv s_0(t) + \xi_0(t). \end{aligned}$$

The signal-to-noise ratio (SNR) at $t = T_0$ is

$$\begin{aligned} \left(\frac{S}{N}\right)^2 &= \frac{s_0^2(T_0)}{E\{\xi_0^2(T_0)\}} = \frac{\left|\int_{-\infty}^{\infty} h(T_0-\tau)s(\tau)d\tau\right|^2}{E\left[\int_{-\infty}^{\infty} h(T_0-\tau)\xi(\tau)d\tau\right]^2} \\ &= \frac{\left|\frac{1}{2\pi}\int_{-\infty}^{\infty} H(\omega)S(\omega)e^{i\omega T_0}d\omega\right|^2}{\frac{1}{2\pi}\int_{-\infty}^{\infty}|H(\omega)|^2 P_\xi(\omega)d\omega} \\ &\leqslant \frac{1}{2\pi}\int_{-\infty}^{\infty}\frac{|S(\omega)|^2}{P_\xi(\omega)}d\omega \\ &= \frac{1}{2\pi}\int_{-\infty}^{\infty}|S(\omega)|^2 d\omega, \end{aligned}$$

where $S(\omega) = \int_{-\infty}^{\infty} s(t)e^{-i\omega t}dt$ and $H(\omega) = \int_{-\infty}^{\infty} h(t)e^{-i\omega t}dt$ are the frequency spectrum of the signal and the transfer function of the filter, respectively. In the above derivation, Parseval's theorem and the Cauchy-Schwartz inequality $|\int_{-\infty}^{\infty} f(x)g(x)dx|^2 \leqslant [\int_{-\infty}^{\infty}|f(x)|^2dx][\int_{-\infty}^{\infty}|g(x)|^2dx]$ were used. Here, the equality holds if and only if $f(x) = g(x)$, which implies that the maximum SNR can be obtained if and only if

$$H(\omega) = S(-\omega)\exp(-i\omega T_0).$$

The best impulse response of the filter is

$$h(t) = \int_{-\infty}^{\infty} S(\omega)\exp[-i\omega(T_0 - t)]d\omega = s(T_0 - t).$$

Thus the green part in Fig. 1 filters the signal by multiplying the time-delayed Rabi reference.

[1] John Van de Vegte, *Feedback Control Systems* (Prentice Hall, New York, 1993).
[2] L. DiCarlo, M. D. Reed, L. Sun, B. R. Johnson, J. M. Chow, J. M. Gambetta, L. Frunzio, S. M. Girvin, M. H. Devoret, and R. J. Schoelkopf, Nature (London) **467**, 574 (2010).
[3] W. Cui, N. Lambert, Y. Ota, X. Y. Lü, Z. L. Xiang, J. Q. You, and F. Nori, Phys. Rev. A **86**, 052320 (2012).
[4] J. Gough and M. R. James, Commun. Math. Phys. **287**, 1109 (2009).
[5] R. Hamerly and H. Mabuchi, Phys. Rev. Lett. **109**, 173602 (2012).
[6] J. Zhang, R. B. Wu, Y. X. Liu, C. W. Li, and T. J. Tarn, IEEE Trans. Autom. Control **57**, 1997 (2012).
[7] S. B. Xue, R. B. Wu, W. M. Zhang, J. Zhang, C. W. Li, and T. J. Tarn, Phys. Rev. A **86**, 052304 (2012).
[8] H. M. Wiseman and G. J. Milburn, Phys. Rev. A **47**, 1652 (1993).
[9] H. M. Wiseman and G. J. Milburn, *Quantum Measurement and Control* (Cambridge University Press, Cambridge, 2009).
[10] J. E. Reiner, W. P. Smith, L. A. Orozco, H. M. Wiseman, and J. Gambetta, Phys. Rev. A **70**, 023819 (2004).
[11] C. Sayrin, I. Dotsenko, Z. Zhou, B. Peaudecerf, T. Rybarczyk, S. Gleyzes, P. Rouchon, M. Mirrahimi, H. Amini, M. Bruner, J. M. Raimond, and S. Haroche, Nature (London) **477**, 73 (2011).
[12] H. Yonezawa, D. Nakane, T. A. Wheatley, K. Iwasawa, S. Takeda, H. Arao, K. Ohki, K. Tsumura, D. W. Berry, T. C. Ralph, H. M. Wiseman, E. H. Huntington, and A. Furusawa, Science **337**, 1514 (2012).
[13] D. Ristè, C. C. Bultink, K. W. Lehnert, and L. DiCarlo, Phys. Rev. Lett. **109**, 240502 (2012).
[14] B. Qi, Automatica **49**, 834 (2013).
[15] J. Q. You and F. Nori, Phys. Today **58**(11), 42 (2005).
[16] R. J. Schoelkopf and S. M. Girvin, Nature (London) **451**, 664 (2008).
[17] J. Q. You and F. Nori, Nature (London) **474**, 589 (2011).
[18] I. Buluta, S. Ashhab, and F. Nori, Rep. Prog. Phys. **74**, 104401 (2011).
[19] Z. L. Xiang, S. Ashhab, J. Q. You, and F. Nori, Rev. Mod. Phys. **85**, 623 (2013).

[20] M. Hatridge, S. Shankar, M. Mirrahimi, F. Schackert, K. Geerlings, T. Brecht, K. M. Sliwa, B. Abdo, L. Frunzio, S. M. Girvin, R. J. Schoelkopf, and M. H. Devoret, Science **339**, 178 (2013).
[21] W. Feng, P. Wang, X. Ding, L. Xu, and X. Q. Li, Phys. Rev. A **83**, 042313 (2011).
[22] M. D. Reed, L. DiCarlo, B. R. Johnson, L. Sun, D. I. Schuster, L. Frunzio, and R. J. Schoelkopf, Phys. Rev. Lett. **105**, 173601 (2010).
[23] D. H. Slichter, R. Vijay, S. J. Weber, S. Boutin, M. Boissonneault, J. M. Gambetta, A. Blais, and I. Siddiqi, Phys. Rev. Lett. **109**, 153601 (2012).
[24] F. Mallet, F. R. Ong, A. P. Laloy, F. Nguyen, P. Bertet, D. Vion, and D. Esteve, Nat. Phys. **5**, 791 (2009).
[25] F. R. Ong, M. Boissonneault, F. Mallet, A. Palacios-Laloy, A. Dewes, A. C. Doherty, A. Blais, P. Bertet, D. Vion, and D. Esteve, Phys. Rev. Lett. **106**, 167002 (2011).
[26] M. Sarovar, H. S. Goan, T. P. Spiller, and G. J. Milburn, Phys. Rev. A **72**, 062327 (2005).
[27] L. Tornberg and G. Johansson, Phys. Rev. A **82**, 012329 (2010).
[28] M. J. Woolley, A. C. Doherty, and G. J. Milburn, Phys. Rev. B **82**, 094511 (2010).
[29] R. Bianchetti, S. Filipp, M. Baur, J. M. Fink, C. Lang, L. Steffen, M. Boissonneault, A. Blais, and A. Wallraff, Phys. Rev. Lett. **105**, 223601 (2010).
[30] A. Frisk Kockum, L. Tornberg, and G. Johansson, Phys. Rev. A **85**, 052318 (2012).
[31] A. N. Korotkov, Phys. Rev. B **71**, 201305(R) (2005).
[32] S. S. Szigeti, S. J. Adlong, M. R. Hush, A. R. R. Carvalho, and J. J. Hope, Phys. Rev. A **87**, 013626 (2013).
[33] R. Vijay, C. Macklin, D. H. Slichter, S. J. Weber, K. W. Murch, R. Naik, A. N. Korotkov, and I. Siddiqi, Nature (London) **490**, 77 (2012).
[34] M. Mirrahimi, B. Buard, and M. Devoret, in *Proceedings of the 51st IEEE Conference on Decision and Control* (IEEE, New York, 2012), pp. 3646–3651.
[35] P. Campagne-Ibarcq, E. Flurin, N. Roch, D. Darson, P. Morfin, M. Mirrahimi, M. H. Devoret, F. Mallet, and B. Huard, Phys. Rev. X **3**, 021008 (2013).
[36] J. J. Pla, K. Y. Tan, J. P. Dehollain, W. H. Lim, J. J. L. Morton, F. A. Zwanenburg, D. N. Jamieson, A. S. Dzurak, and A. Morello, Nature (London) **496**, 334 (2013).
[37] K. Lalumière, J. M. Gambetta, and A. Blais, Phys. Rev. A **81**, 040301(R) (2010).
[38] J. Gambetta and H. M. Wiseman, Phys. Rev. A **64**, 042105 (2001).
[39] S. Gammelmark and K. Molmer, Phys. Rev. A **87**, 032115 (2013).
[40] M. Christandl and R. Renner, Phys. Rev. Lett. **109**, 120403 (2012).
[41] M. Tsang, Phys. Rev. Lett. **108**, 230401 (2012).
[42] W. D. Oliver, Y. Yu, J. C. Lee, K. L. Berggren, L. S. Levitov, and T. P. Orlando, Science **310**, 1653 (2005).
[43] Y. Yin, Y. Chen, D. Sank, P. J. J. O'Malley, T. C. White, R. Barends, J. Kelly, E. Lucero, M. Mariantoni, A. Megrant, C. Neill, A. Vainsencher, J. Wenner, A. N. Korotkov, A. N. Cleland, and J. M. Martinis, Phys. Rev. Lett. **110**, 107001 (2013).
[44] K. W. Murch, U. Vool, D. Zhou, S. J. Weber, S. M. Girvin, and I. Siddiqi, Phys. Rev. Lett. **109**, 183602 (2012).
[45] Z. Liu, L. Kuang, K. Hu, L. Xu, S. Wei, L. Guo, and X. Q. Li, Phys. Rev. A **82**, 032335 (2010).
[46] J. Gambetta, A. Blais, M. Boissonneault, A. A. Houck, D. I. Schuster, and S. M. Girvin, Phys. Rev. A **77**, 012112 (2008).
[47] A. Blais, J. Gambetta, A. Wallraff, D. I. Schuster, S. M. Girvin, M. H. Devoret, and R. J. Schoelkopf, Phys. Rev. A **75**, 032329 (2007).
[48] Y. X. Liu, L. F. Wei, and F. Nori, Phys. Rev. B **72**, 014547 (2005).
[49] W. Cui, Z. R. Xi, and Y. Pan, Phys. Rev. A **77**, 032117 (2008).
[50] Y. Pan, Z. R. Xi, and W. Cui, Phys. Rev. A **81**, 022309 (2010).
[51] J. F. Ralph, K. Jacobs, and C. D. Hill, Phys. Rev. A **84**, 052119 (2011).
[52] S. Kuang and S. Cong, Automatica **44**, 98 (2008).
[53] D. Y. Dong and I. R. Petersen, Automatica **48**, 725 (2012).
[54] M. Mirrahimi and G. Turinici, Automatica **41**, 1987 (2005).
[55] X. Wang and S. G. Schirmer, IEEE Trans. Autom. Control **55**, 2259 (2010).
[56] X. X. Yi, X. L. Huang, C. Wu, and C. H. Oh, Phys. Rev. A **80**, 052316 (2009).
[57] S. C. Hou, M. A. Khan, X. X. Yi, D. Dong, and I. R. Petersen, Phys. Rev. A **86**, 022321 (2012).
[58] H. Amini, R. A. Somaraju, I. Dotsenko, C. Sayrin, M. Mirrahimi, and P. Rouchon, Automatica **49**, 2683 (2013).